DNA Research, 2018, 25(3), 277–286
doi: 10.1093/dnares/dsx056
Advance Access Publication Date: 17 January 2018
Full Paper

OXFORD

Full Paper

Transcriptome profiling reveals infection strategy of an insect maculavirus

Susumu Katsuma[1,*,†], Munetaka Kawamoto[1,†], Keisuke Shoji[1,2,†], Takahiro Aizawa[2,†], Takashi Kiuchi[1], Natsuko Izumi[3], Moe Ogawa[2], Takaaki Mashiko[4], Hideki Kawasaki[2], Sumio Sugano[5], Yukihide Tomari[3,6], Yutaka Suzuki[7], and Masashi Iwanaga[2,*]

[1]Department of Agricultural and Environmental Biology, Graduate School of Agricultural and Life Sciences, The University of Tokyo, Bunkyo-ku, Tokyo 113-8657, Japan, [2]Department of Agrobiology and Bioresources, School of Agriculture, Utsunomiya University, Utsunomiya-shi, Tochigi 321-8505, Japan, [3]Institute of Molecular and Cellular Biosciences, The University of Tokyo, Bunkyo-ku, Tokyo 113-0032, Japan, [4]Department of Biological Production Science, United Graduate School of Agricultural Science, Tokyo University of Agriculture and Technology, Fuchu-shi, Tokyo 183-8509, Japan, [5]Department of Computational Biology and Medical Sciences, Graduate School of Frontier Sciences, The University of Tokyo, Minato-ku, Tokyo 108-8639, Japan, [6]Department of Computational Biology and Medical Sciences, Graduate School of Frontier Sciences, The University of Tokyo, Bunkyo-ku, Tokyo 113-0032, Japan, and [7]Department of Computational Biology and Medical Sciences, Graduate School of Frontier Sciences, The University of Tokyo, Kashiwa, Chiba 277-0882, Japan

*To whom correspondence should be addressed. Tel. +81-3-5841-8994. Fax. +81-3-5841-8993. Email: katsuma@ss.ab.a.u-tokyo.ac.jp (S.K.); Tel. +81-28-649-5454. Fax. +81-28-649-5401. Email: iwanaga@cc.utsunomiya-u.ac.jp (M.I.)
†These authors contributed equally to this work.

Edited by Dr Yuji Kohara

Received 21 September 2017; Editorial decision 25 December 2017; Accepted 3 January 2018

Abstract

Bombyx mori macula-like virus (BmMLV) is a positive, single-stranded insect RNA virus that is closely related to plant maculaviruses. BmMLV is currently characterized as an unclassified maculavirus. BmMLV accumulates at extremely high levels in cell lines derived from the silkworm, *Bombyx mori*, but it does not lead to lethality and establishes persistent infections. It is unknown how this insect maculavirus replicates and establishes persistent infections in insect cells. Here, we showed that BmMLV *p15*, which is located on a subgenomic fragment and is not found in plant maculaviruses, is highly expressed in BmMLV-infected silkworm cells and that p15 protein is required to establish BmMLV infections in silkworm cells. We also showed that two distinct small RNA-mediated pathways maintain BmMLV levels in BmMLV-infected silkworm cells, thereby allowing the virus to establish persistent infection. Virus-derived siRNAs and piRNAs were both produced as the infection progressed. Knockdown experiments demonstrated that the exogenous RNAi pathway alone or RNAi and piRNA pathways function cooperatively to silence BmMLV RNA and that both pathways are important for normal growth of BmMLV-infected silkworm cells. On the basis of our study, we propose a mechanism of how a plant virus-like insect virus can establish persistent infections in insect cells.

Key words: maculavirus, silkworm, piRNA, siRNA, persistent infection

1. Introduction

Maculavirus is a plant virus typified by Grapevine fleck virus (GFkV).[1] The genome of GFkV is a 7,564-base-long single-stranded RNA containing four putative open reading frames each of which encodes replicase (RdRp), coat protein (CP) and one or two proline-rich proteins with unknown functions. The RdRp and CP are phylogenetically related to the corresponding proteins found in members of the genera *Tymovirus* and *Marafivirus*. The host range of maculaviruses is restricted to European and American *Vitis* species, but their vectors have not been identified.

In 2005, we identified a 2,379-base-long cDNA clone from the cDNA library of the silkworm *Bombyx mori* ovary-derived BmN-4 cell line, which had significant homology to the *rdrp* and *cp* genes of GFkV.[2] Northern blot analysis showed that two transcripts of 6.5 and 1.3 kb are expressed in BmN-4 cells and the shorter transcript is likely a subgenomic fragment containing the *cp* gene. Cloning and sequencing of the full-length 6,519-base-long cDNA revealed that this RNA contains three putative genes: *rdrp*, *cp* and *p15*. The putative p15 protein does not show significant homology with any known proteins, although the RdRp and CP exhibited high homology to those of GFkV. Virus-like particles containing this maculavirus-like RNA were purified from BmN-4 cells and isometric virions 28 to 30 nm in diameter were observed under electron microscopy. We termed this novel RNA virus *Bombyx mori macula-like virus* (BmMLV). BmMLV is currently characterized as an unclassified maculavirus.[3]

BmMLV was detected in seven out of eight cell lines derived from *B. mori*, but not from two other lepidopteran cell lines *Spodoptera frugiperda* Sf-9 and *Trichoplusia ni* High Five.[2] Infection studies revealed that persistent infections with BmMLV are not established in Sf-9 cells.[4] The level of BmMLV *cp* RNA in BmN-4 cells is comparable to that of a housekeeping gene *Actin3* in BmN-4 cells,[2] indicating that BmMLV accumulated at extremely high levels in persistently infected silkworm cells. Recently, we found *B. mori* embryo-derived VF cells that have not been infected with BmMLV.[5] We successfully established VF cells persistently infected with BmMLV (designated as VF-MLV) without strong cytopathic effects, suggesting that BmMLV has a potential to establish persistent infections in silkworm cells. At present, however, it is unknown how this 'insect' maculavirus replicates and establishes persistent infections only in silkworm cells.

In this study, we performed transcriptome analysis of silkworm cells acutely or persistently infected with BmMLV and found that BmMLV *p15* is highly expressed in BmMLV-infected cells. Further experiments using infectious cDNA clones showed that p15 is essential for establishing BmMLV infections in silkworm cells. In addition, we observed a gradual decrease in BmMLV RNA during the establishment of persistent infections. Small RNA sequencing and knockdown experiments revealed that BmMLV RNA-derived small interfering RNAs (vsiRNAs) and PIWI-interacting RNAs (vpiRNAs) play essential roles in establishing persistent infections in silkworm cells.

2. Materials and methods

2.1. Cell lines

BmN-4 cells (provided by Chisa Yasunaga-Aoki, Kyushu University, and maintained in our laboratory)[6] were cultured at 27°C in IPL-41 medium (Applichem) supplemented with 10% fetal bovine serum. VF and VF-MLV cells (established and maintained in our laboratory) were cultured at 27°C in IPL-41 medium (Applichem) supplemented with gamma ray-treated 10% fetal bovine serum.[5]

2.2. Transfection and Western blotting

Transfection of VF cells with BmMLV infectious clones and Western blotting with anti-CP and Actin antibodies were performed as described previously.[5] cDNA clones pHMLV-Δp15 and pHMLV-p15ΔMet + Stop were generated with a KOD -plus- Mutagenesis Kit (TOYOBO) using pHMLV[5] as a template.

2.3. RNA-seq

RNA-seq experiments were performed as described previously.[7] RNA-seq libraries were generated from total RNA samples prepared from BmMLV-infected VF cells at 0, 6, 12, 24, 48 and 96 h post-infection (hpi) and 2 weeks post-infection (wpi), and from VF-MLV cells using the TruSeq RNA Sample Preparation Kit (Illumina). The libraries were analysed by the Illumina HiSeq 2500 platform based on 100-bp paired-end reads according to the manufacturer's protocol. *De novo* assembly of RNA-seq data from eight data sets was performed using Trinity.[8] The transcript abundance in each contig was quantified by RSEM.[9] Differentially expressed genes (DEGs, $P < 0.005$) between 0 hpi and other samples were identified by DESeq.[10] We selected 150 DEGs with more than 30 transcripts per million in any data set. Raw RNA-seq data were also mapped to the BmMLV genome by TopHat2.[11] Clustering analysis was performed as described previously.[12]

2.4. Sequence analysis of cloned small RNAs

Cloning and sequencing of Siwi- and BmAgo3-bound BmN-4 piRNAs were performed as described previously.[13] VF cells were infected with BmMLV[5] and small RNA libraries were constructed using a Small RNA Cloning Kit (TaKaRa) and sequenced using the Illumina HiSeq 2500 platform. Informatics analysis of small RNAs was performed as reported previously.[14] In brief, The 3′-adaptor sequences were identified and removed, allowing for up to two mismatches. Reads shorter than 20 nucleotides (nt) or longer than 32 nt were excluded, thereby obtaining reads of 20–32 nt. Mapping small RNAs to the *Bombyx* genome[15] was performed using bowtie.[16] Reads that could be aligned to the genome up to two mismatches were used to calculate the mapping rate of each library. Mapping rates against the genome were used for normalization. Sam files were converted to bam files by SAMtools,[17] then to bed files, and the coverage of each nucleotides was calculated by BEDTools.[18]

2.5. RNA interference (RNAi) in BmN-4, VF and VF-MLV cells

RNAi experiments in BmN-4 cells were performed as described previously.[19] VF and VF-MLV cells (2.5×10^5 cells per 35-mm diameter dish) were transfected with siRNAs (250 pmol per dish) using X-tremeGENE HP (Roche). Transfection was performed twice at 72 h intervals. VF cells were infected with BmMLV during the second transfection. Total RNA was isolated at 96 h after the second transfection.

2.6. Reverse transcription-quantitative polymerase chain reaction (RT-qPCR)

To validate the RNA-seq analysis (Supplementary Figs S1 and S2A), total RNA was reverse transcribed by PrimeScript™ RT reagent Kit (TaKaRa) and RT-qPCR was performed with SYBR Premix ExTaq

II (Tli RNaseH Plus). For the RT-qPCR experiments shown in Figs 4A–C, 5A–B, Supplementary Figs S5A–B, S5D, S6A–B and S7A, the total RNA was subjected to reverse transcription with avian myeloblastosis virus reverse transcriptase and oligo-dT primer (TaKaRa). RT-qPCR was performed using a KAPA SYBR FAST qPCR Kit (Kapa Biosystems) and the specific primers listed in Supplementary Table S2. The expression values were calculated using the 2^{-Ct} method. The value of each transcript in control cells was considered to be 100 and the relative levels of transcripts in treated cells were estimated.

2.7. *Agrobacterium* coinfiltration leaf patch assay

BmMLV *p15* cDNA was amplified using primers p15_supp_F and p15_supp_R from the BmMLV full-length cDNA clone pHMLV, and cloned into the pE7133 vector (pE7133-P15).[20] The plasmid pE7133-HC-Pro was also generated by inserting the *helper component-protease* (*HC-Pro*) gene of *Zucchini yellow mosaic virus* (ZYMV) Z5 isolate.[21] Subsequently, the fragments between E7 (35S promoter upstream sequence of the cauliflower mosaic virus) and Tnos (polyadenylation signal of the gene for nopaline synthase) of pE7133-P15, pE7133-HC-Pro and pE7133-GUS[20] were subcloned into the *Agrobacterium* binary vector pCAMBIA2300[22] (designated 35S-P15, 35S-HC-Pro and 35S-GUS, respectively). Each of the constructs was transformed into *Agrobacterium tumefaciens* strain GV2260. *Agrobacterium* cultures harboring 35S-GFP and 35S-P15, 35S-HC-Pro or 35S-GUS were mixed in equal proportions and coinfiltrated into the *Nicotiana benthamiana* 16c leaves.[23] After 5 days of postinfiltration, GFP fluorescence was observed and photographed using a fluorescence microscope (M205 FA, Leica) with a cooled CCD camera (DFC450 C, Leica).

2.8. Accession numbers

The deep sequencing data obtained in this study are available under the accession numbers DRA003575 (RNA-seq), DRA005085–DRA005087 (piRNA-seq).

3. Results and discussion

BmMLV belongs to the plant virus genus *Maculavirus*, but this virus propagates to a massive extent in silkworm cells and establishes persistent infections without strong cytopathic effects.[2,5] To understand the molecular interaction between this plant virus-like virus and insect cells, we performed RNA-seq experiments using BmMLV and *B. mori* embryo-derived BmMLV-free VF cells.[5] We used total RNA samples prepared from BmMLV-infected VF cells at 0, 6, 12, 24, 48 and 96 hpi and at 2 wpi. We also performed RNA-seq analysis using VF cells that had been persistently infected with BmMLV for more than 2 years (VF-MLV).[5] We selected 150 DEGs ($P < 0.005$) between 0 hpi and other samples by DESeq and classified them into 10 clusters based on their expression patterns (Fig. 1A and B and Supplementary Table S1). The expression patterns of some DEGs were verified in RT-qPCR experiments (Supplementary Figs S1 and S2A). Clusters A–F included DEGs with expression levels that transiently increased following BmMLV infection, but remained at basal levels in VF-MLV cells. The expression levels of the DEGs in clusters A, C and D were higher at 2 wpi than at 0 hpi, whereas the DEGs in clusters B and F declined rapidly at 24 hpi and 2 wpi, respectively and then remained at the basal level. Cluster G was the largest cluster and contained 37 genes encoding transcription factors, enzymes and heat shock proteins. The expression of cluster G genes gradually decreased until 96 hpi and they returned to the basal levels in VF-MLV cells. The DEGs in clusters H and I were up-regulated during transient infection and they remained at high levels in VF-MLV cells. Cluster J contained 21 DEGs with markedly higher expression in persistently infected VF-MLV cells than in acutely infected cells. Two genes, *Dscam* and *fasciclin*, which have been shown to function in cell adhesion,[24,25] were included in this cluster. RT-qPCR verified the gradual increases in the *Dscam* and *fasciclin* mRNA levels and their high expression levels in VF cells at 2 wpi as well as in VF-MLV cells (Supplementary Fig. S2A). Up-regulation of these cell adhesion molecules might lead to the formation of cell aggregates, which were observed frequently during BmMLV infection (Supplementary Fig. S2B). Transcriptome analysis showed that the changes in the mRNA levels of most genes were transient, i.e. the mRNA levels returned to the basal level in the persistent infection stage, whereas the expression levels of a small number of genes, such as cell adhesion molecules, were enhanced and they remained higher even in persistently infected cells.

RNA-seq analysis determined the detailed growth pattern of BmMLV in VF cells. Mapping of RNA-seq reads onto the BmMLV sequence detected BmMLV replication from 24 hpi and rapid propagation from 48 hpi. The growth peaked at 96 hpi and decreased slightly at 2 wpi (Fig. 2A and Supplementary Fig. S3A). In persistently infected VF-MLV cells, the BmMLV RNA level declined to about 60% of that found in BmMLV-infected VF cells at 96 hpi (Fig. 2A). These results demonstrate that BmMLV replication begins from 24 hpi, progresses rapidly until 96 hpi and then declines gradually during persistent infection. We also observed that subgenomic RNA markedly accumulated during BmMLV infection (Fig. 2B and Supplementary Fig. S3A). The subgenomic RNA is considered to contain two genes *cp* and *p15*.[2] *cp* encodes a CP, but it is unknown whether *p15* actually encodes a functional protein.[2,5] The *p15* RNA expression level was much higher than that of *cp* RNA, especially in VF-MLV cells (Fig. 2B and Supplementary Fig. S3A), thereby suggesting that *p15* plays an essential role in the establishment of BmMLV infections in silkworm cells. The putative p15 protein lacks high homology with any known proteins including plant maculavirus proteins, but it shares very low homology (E value = 3e-04) with a hypothetical protein of insect iridovirus (accession number YP_009010649), which suggests that it might be required for infection in insect cells. We established a system where infectious BmMLV virions could be produced via the transfection of VF cells with an infectious BmMLV full-length cDNA clone (pHMLV).[5] To understand the role of *p15* in the establishment of BmMLV infection, we generated two cDNA clones that lacked *p15* (pHMLV-Δp15) or that possessed a Met codon-defective *p15* (pHMLV-p15ΔMet + Stop) (Fig. 2C), and we transfected them into VF cells, before examining virus production in the transfected cells by immunoblotting for the CP protein. We observed CP protein expression in pHMLV-transfected VF cells, whereas we did not detect its expression at all in pHMLV-Δp15- or pHMLV-p15ΔMet + Stop-transfected cells (Fig. 2D). These results demonstrate that p15 protein but not *p15* RNA is required for the establishment of BmMLV infections in silkworm cells.

Plant RNA viruses often encode RNA silencing suppressors in order to counterattack against host antiviral silencing.[26] To investigate whether p15 protein functions as a RNA silencing suppressor, we performed an *Agrobacterium*-mediated transient coexpression assay.[27] In this conventional assay, suppression of transgene-induced RNA silencing in patches infiltrated with *Agrobacterium* cells was examined using GFP fluorescence. A plasmid expressing GFP (35S-GFP) and a plasmid expressing BmMLV p15 (35S-P15) were coinfiltrated into *N. benthamiana* leaves by agroinfiltration. As negative

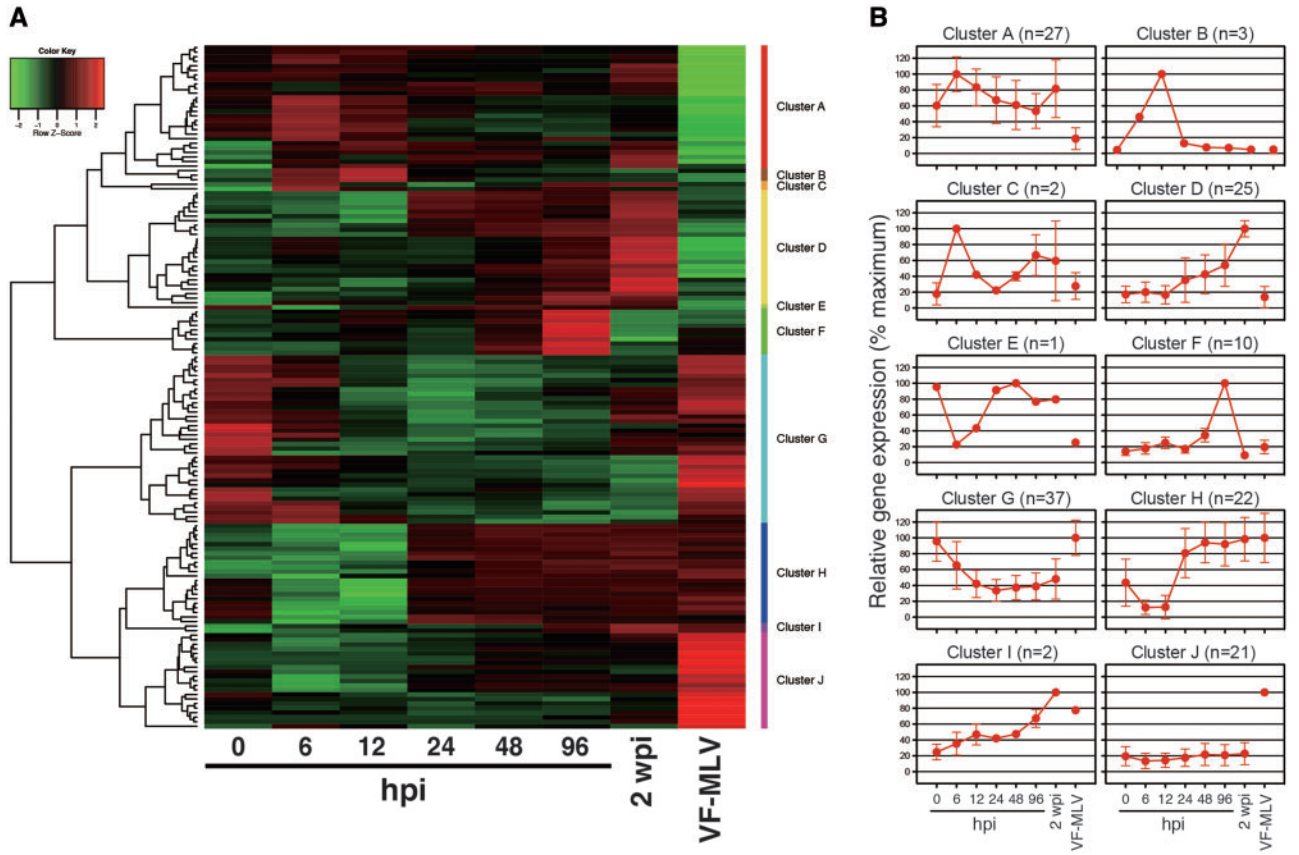

Figure 1. Virus–host interaction during acute and persistent BmMLV infections in silkworm cells. (A) Hierarchical cluster analysis of 150 selected DEGs. The temporal expression profiles of 150 DEGs were hierarchically clustered and visualized as a heat map. RNA-seq experiments for each sample are shown in the columns and the individual genes in rows. (B) Cluster profiles. DEGs were subdivided into 10 clusters. The expression pattern of each cluster is shown as a line graph. The numbers of genes within each cluster are also shown.

and positive controls, either β-glucuronidase (35S-GUS) or the well-characterized RNA silencing suppressor HC-Pro of ZYMV (35S-HC-Pro), respectively, was coexpressed with GFP. As shown in Fig. 2E, coinfiltration with 35S-GFP and 35S-HC-Pro elicited strong green fluorescence as a consequence of suppression of RNA silencing. On the other hand, coinfiltration with 35S-GFP and 35S-P15 or 35S-GUS triggered RNA silencing and resulted in very weak GFP fluorescence (Fig. 2E). These results indicate that BmMLV p15 protein does not work as a viral RNA silencing suppressor in this system. This result, along with the result that CP expression was completely diminished when *p15* of the BmMLV infectious cDNA was mutated or deleted (Fig. 2D), suggested that p15 protein is required for BmMLV replication in silkworm cells. Recent studies have identified additional insect macula-like viruses in mosquitoes, honeybees and mites.[28,29] *Culex* Tymoviridae-like virus (CuTLV) and Bee Macula-like virus (BeeMLV) possess *p16* and *p15* genes, which encode proteins with low sequence identities (16.6% and 17.7%, respectively) to BmMLV p15 protein. On the other hand, mite Varroa Tymo-like virus and plant maculaviruses do not possess *p15* orthologues. These findings suggest that insect macula-like viruses have acquired and utilized their unique genes to replicate in insect hosts, i.e., silkworm cells, mosquitoes and honeybees.

The amount of BmMLV RNA decreased gradually during the establishment of persistent infections in VF cells (Fig. 2A), thereby indicating the existence of a host silencing mechanism against BmMLV. A previous study showed that an RNAi pathway possibly down-regulates the level of BmMLV *rdrp* RNA in the *B. mori* ovary-derived BmN-4 cell line[30] that is known to be persistently infected with BmMLV.[2] Thus exogenous small RNA-mediated pathways might be involved in decreasing BmMLV RNA in persistently infected cells. Since small RNA libraries obtained from BmN-4 cells are available in public databases,[31] a search for BmMLV RNA-derived small RNAs was first made by mapping BmN-4 small RNA sequences onto the BmMLV genome. BmMLV RNA-derived small RNAs were found to be expressed from the entire genomic region (Fig. 3A). These viral small RNAs had a very strong sense-strand bias, and few were mapped to the antisense strand (Fig. 3A and B). The small RNAs mapped to the *rdrp* region varied in length between 20 and 32 nt and they had weak peaks at around 20 nt, which suggests that they belonged to microRNAs (miRNAs) or small interfering RNAs (siRNAs). miRNAs and siRNAs play biological roles by cooperating with Ago1 and Ago2 proteins, respectively.[32] We examined the properties of BmMLV-derived Ago2-bound small RNAs using a small RNA library obtained from BmN-4 cells infected with an Ago2-overexpressing baculovirus.[33] They were mapped to both strands with a weak sense-strand bias (Fig. 3A), and had a distinct peak at 20 nt (Fig. 3C). Although this data set was obtained under a different condition from ours, bioinformatic analysis indicates that Ago2-bound small RNAs contain BmMLV-derived siRNAs (vsiRNAs), which are produced from double-stranded BmMLV RNA-derived precursor RNAs. In addition, a distinct peak in the length distribution of small RNAs mapped to the *cp* and *p15* regions

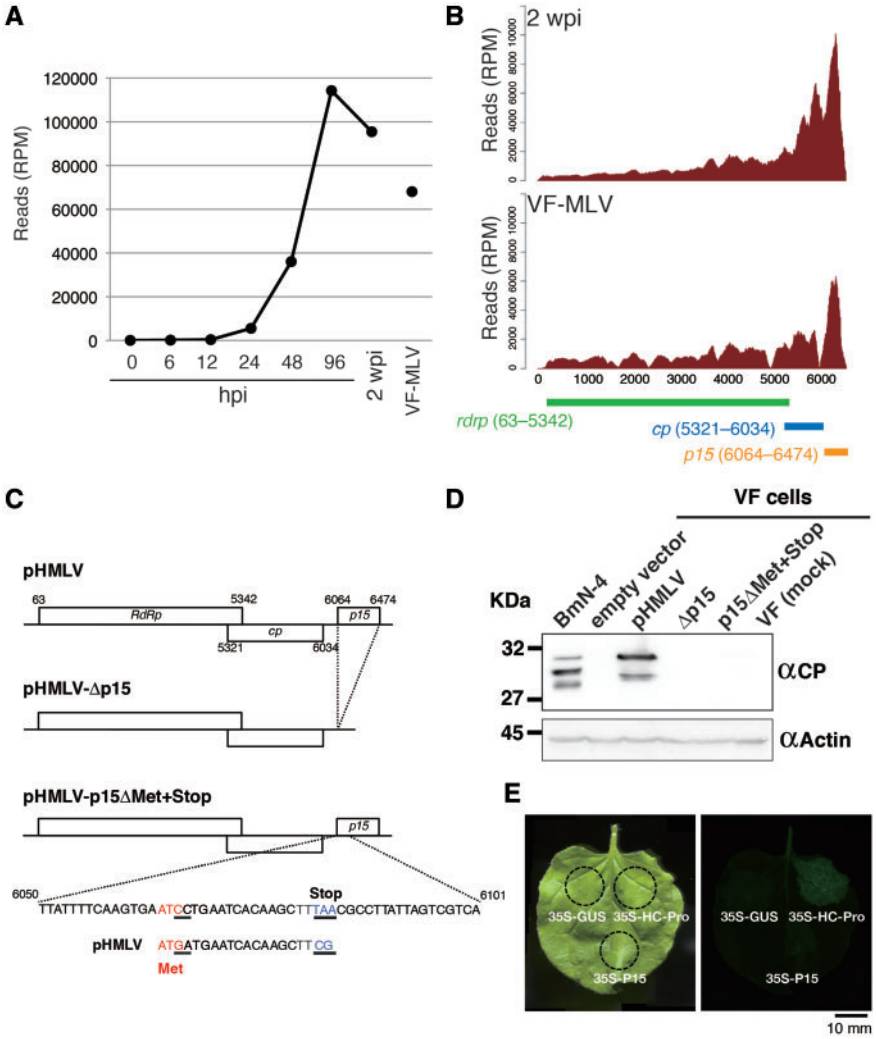

Figure 2. p15 is essential for establishing BmMLV infections in silkworm cells. (A) Accumulation profile of BmMLV RNA in VF cells. (B) Mapping of RNA-seq reads onto the BmMLV sequence. The location of each gene is also shown. (C) Schematic representation of BmMLV cDNA clones. pHMLV is an infectious cDNA clone of BmMLV. pHMLV-Δp15 completely lacks the *p15* region, whereas pHMLV-p15ΔMet + Stop possesses a mutation in the Met codon and the insertion of a stop codon. (D) Immunoblot detection of CP. VF cells were transfected with the empty vector, pHMLV or pHMLV derivatives and subjected to Western blotting with anti-CP antibody. BmN-4 and VF (mock) cells were used as positive and negative controls, respectively. Actin is shown as a loading control. (E) GFP fluorescence of *N. benthamiana* leaves infiltrated with *Agrobacterium* mixtures containing a vector expressing GFP (35S-GFP) and BmMLV p15 (35S-P15), ZYMV HC-Pro (35S-HC-Pro) or β-glucuronidase (35S-GUS). The GFP fluorescence was photographed under UV light at 5 days postinfiltration.

was observed at 27–28 nt (Fig. 3B), which was similar to that observed in the total small RNAs obtained from naïve BmN-4 cells.[13,34] These small RNAs are probably piRNAs that repress transposon activity by cooperating with silkworm PIWI proteins, Siwi and BmAgo3.[34,35] In the silkworm piRNA biogenesis pathway called 'ping-pong' cycle, Siwi and 1U piRNA complexes cleave their complementary targets across from nts 10 and 11 from the guide piRNAs.[34] The cleaved 3′ RNA fragments are subsequently incorporated into another PIWI protein BmAgo3 and processed into mature secondary piRNAs with adenine at the position 10 (10A), which precisely overlap with 1U piRNAs by 10 nt. To determine whether BmMLV RNA-derived piRNAs (vpiRNAs) were loaded correctly into PIWI proteins, we sequenced Siwi-bound or BmAgo3-bound small RNAs from BmN-4 cells and mapped them onto the BmMLV genome (Fig. 3A). In contrast to the mapping results obtained for the total small RNAs, the Siwi-bound and BmAgo3-bound vpiRNAs mapped exclusively to the subgenomic region, where *cp* and *p15* are encoded (Fig. 3A). The Siwi- and BmAgo3-bound vpiRNAs had a very strong sense-strand bias, and a small proportion of BmAgo3-bound vpiRNAs were mapped to the antisense strand of the subgenomic region (Fig. 3A). Siwi-bound and BmAgo3-bound vpiRNAs had peak length distribution of 28 and 27 nt, respectively (Fig. 3D and E), which are identical to those observed in transposon-derived piRNAs in BmN-4 cells.[13] The Siwi-bound sense vpiRNAs exhibited 1U enrichment, whereas the BmAgo3-bound vpiRNAs lacked this bias (Supplementary Fig. S4). Intriguingly, 10A enrichment was observed in both Siwi- and BmAgo3-bound antisense vpiRNAs (Supplementary Fig. S4), which suggests that some of the vpiRNAs are produced via the Siwi : Siwi homotypic ping-pong cycle, instead of the canonical Siwi : BmAgo3 heterotypic ping-pong cycle. This unique biogenesis feature might result in an extremely strong sense-strand bias in BmMLV vpiRNAs (Fig. 3A).

To determine the small RNA pathways that are involved in the silencing of BmMLV RNA in BmN-4 cells, we performed knockdown

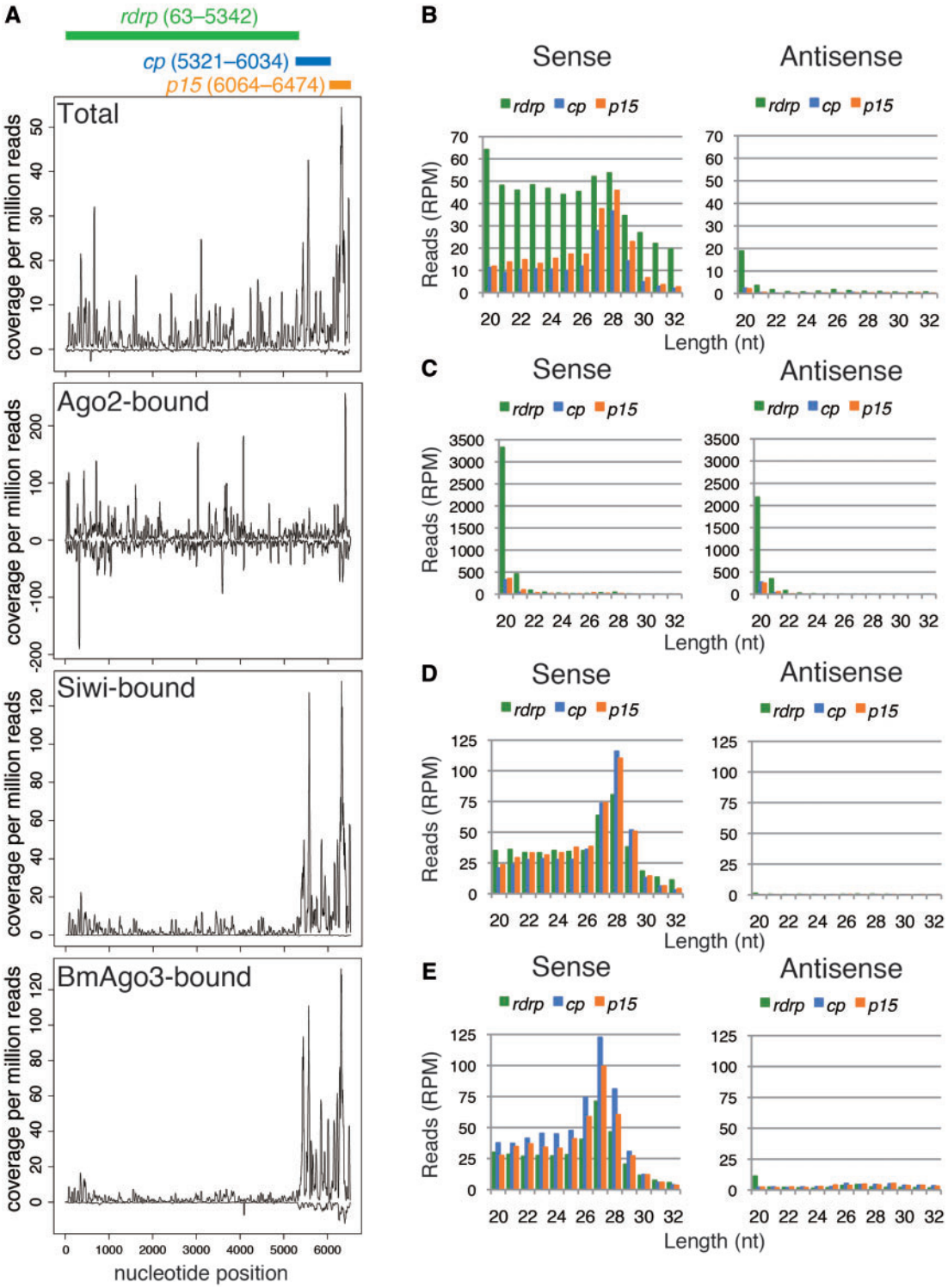

Figure 3. Production of BmMLV-derived small RNAs in BmN-4 cells. (A) Mapping of BmN-4 small RNAs onto the BmMLV sequence. Total piRNA data were from DRA003745.[31] Ago2-bound small RNA data were from SRR609266.[33] (B–E) Length distribution of BmMLV RNA-derived small RNAs in the total (B), Ago2-bound (C), Siwi-IPed (D) and BmAgo3-IPed (E) piRNA libraries.

experiments against all four silkworm *Ago* family genes, *Ago1*, *Ago2*, *Siwi* and *BmAgo3*. Ago1 and Ago2 proteins are required for the miRNA- and siRNA-mediated pathways,[32] respectively, whereas Siwi and BmAgo3 are core components of the piRNA machinery in silkworms.[34,35] First, we knocked down *Siwi* or *BmAgo3* mRNA in BmN-4 cells, where the knockdown efficiency was verified by RT-qPCR experiments (Supplementary Fig. S5A). As shown in Fig. 4A, the RNA levels of *rdrp* and *cp* were higher in *Siwi*- or *BmAgo3*-knocked down cells compared with those in the control cells, thereby demonstrating that vpiRNAs are involved in the suppression of BmMLV propagation

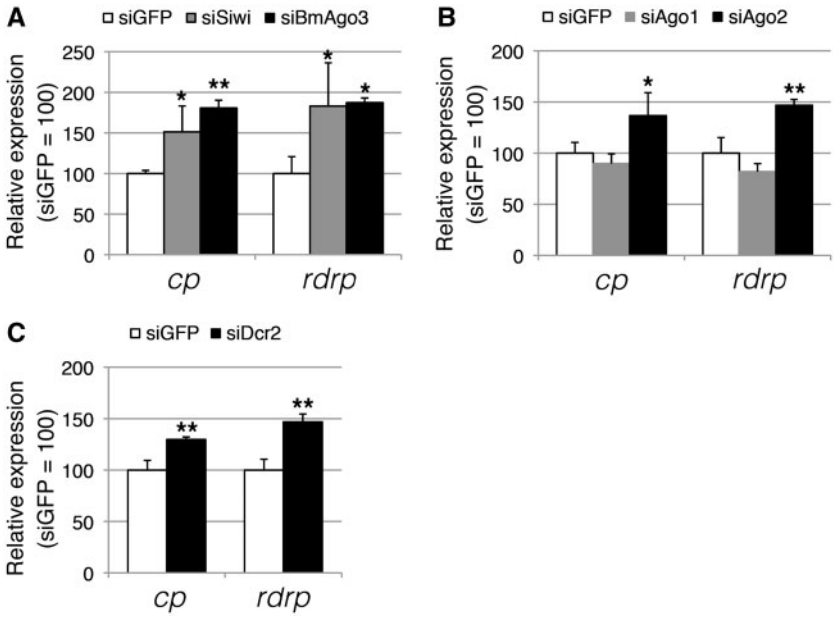

Figure 4. Exogenous piRNA and RNAi pathways cooperatively suppress BmMLV replication in BmN-4 cells. (A) Expression of *cp* and *rdrp* RNAs in *Siwi*- or *BmAgo3*-knocked down BmN-4 cells. (B) Expression of *cp* and *rdrp* RNAs in *Ago1*- or *Ago2*-knocked down BmN-4 cells. Data represent the mean ± standard deviation (SD) of triplicates. $*P<0.05$, $**P<0.01$ by one-way analyses of variance (ANOVA) and Dunnett's posttests using siGFP as a control. (C) Expression of *cp* and *rdrp* RNAs in *Dcr2*-knocked down BmN-4 cells. Data represent the mean ± SD of triplicates. $**P<0.01$ by two-tailed *t*-test.

in BmN-4 cells. Furthermore, we knocked down *Ago1* or *Ago2* mRNA (Supplementary Fig. S5B) and examined the expression levels of *rdrp* and *cp* in the knocked down cells. We observed enhancement of both the *rdrp* and *cp* RNA levels in the *Ago2*-knocked down cells, but knocking down *Ago1* mRNA did not affect the levels of BmMLV RNAs (Fig. 4B). To verify whether exogenous siRNA pathway is involved in BmMLV suppression, we knocked down *Dicer-2* (*Dcr2*) which makes siRNAs from long double-stranded RNAs. As shown in Fig. 4C and Supplementary Fig. S5D, we detected *cp* and *rdrp* increase in *Dcr2*-knocked down cells. These results demonstrate that BmMLV replication is suppressed by exogenous piRNA- and siRNA-mediated pathways in BmMLV persistently infected BmN-4 cells. We also observed cell growth inhibition or reduced cell viability in *Ago2*-, *Siwi*-, *BmAgo3*- or *Dcr2*-knocked down cells (Supplementary Fig. S5C and E). Considering that the percentage of BmMLV RNA-derived RNA-seq reads was surprisingly high, i.e. more than 15% of the total reads in BmN-4 cells (Supplementary Fig. S3B), a few fold increase in the intracellular amounts of BmMLV might be fatal for the growth and viability of BmN-4 cells.

Next, we investigated whether both vpiRNAs and vsiRNAs are also involved in the suppression of BmMLV replication in BmMLV-free VF cells. We knocked down four *Ago* family genes and then infected the knocked down VF cells with BmMLV. The RNA levels of *cp* and *rdrp* were enhanced only when *Ago2* was knocked down (Fig. 5A and Supplementary Fig. S6A). These results clearly demonstrate that BmMLV is repressed by the siRNA pathway, but not by the piRNA pathway in VF cells when transiently infected with BmMLV. To examine whether the siRNA pathway alone mediates BmMLV suppression in VF cells persistently infected with BmMLV, we knocked down each *Ago* family gene in VF-MLV cells (Supplementary Fig. S6B) and examined the *cp* and *rdrp* levels in the knocked down cells. We found that the amount of BmMLV RNA was enhanced only in *Ago2*-knocked down VF-MLV cells (Fig. 5B), thereby indicating the involvement of the siRNA pathway, but not the piRNA pathway, in the repression of BmMLV replication in VF-MLV cells. Next, we sequenced small RNAs from BmMLV-infected VF cells (0, 24 and 96 hpi) and VF-MLV cells. Few small RNAs obtained from BmMLV-infected VF cells at 0 or 24 hpi mapped to the BmMLV genome (Fig. 5C). At 96 hpi, the BmMLV RNA-derived small RNAs mapped to the entire BmMLV genome and they exhibited a weak sense-strand bias (Fig. 5C). The peak of the length distribution of these small RNAs was 20–21 nt (Fig. 5D–F), thereby suggesting that they were siRNAs or miRNAs. Given the results of the knockdown experiments (Fig. 5A and B), these small RNAs were vsiRNAs. In addition, we sequenced small RNAs prepared from VF-MLV cells and found that the mapping pattern differed markedly from that of BmN-4 cells (Fig. 3A). The peak of the length distribution of these small RNAs was 20–21 nt and a faint broad peak ranging between 26 and 30 nt was observed for both strands (Fig. 5G), which suggests that vpiRNAs accumulated at much lower levels compared with the vsiRNAs in VF-MLV cells. These results confirmed our observation that BmMLV was repressed by the siRNA-mediated pathway but not by the piRNA-mediated pathway in both transiently and persistently infected VF cells (Fig. 5A and B).

Two possible mechanisms may explain the different silencing strategies observed in the two silkworm cell lines. First, these two cell lines might simply possess different silencing pathways against foreign elements. BmN-4 is derived from the *B. mori* ovary[6] and it possesses a complete piRNA pathway.[34] On the other hand, VF was established from *B. mori* early embryos,[5] but it is unknown whether this cell line possesses the piRNA pathway. Bioinformatics analysis showed that the VF cells actually expressed both piRNA pathway-related genes and transposon-derived piRNAs (data not shown), and thus VF cells also have the potential for piRNA-mediated silencing. Therefore, a second hypothesis is possible, which involves the difference in the virus accumulation level in the two cell lines. BmMLV RNA-derived reads accounted for 15.7% and 8.3% of the total RNA-seq reads in BmN-4 and VF-MLV cells, respectively

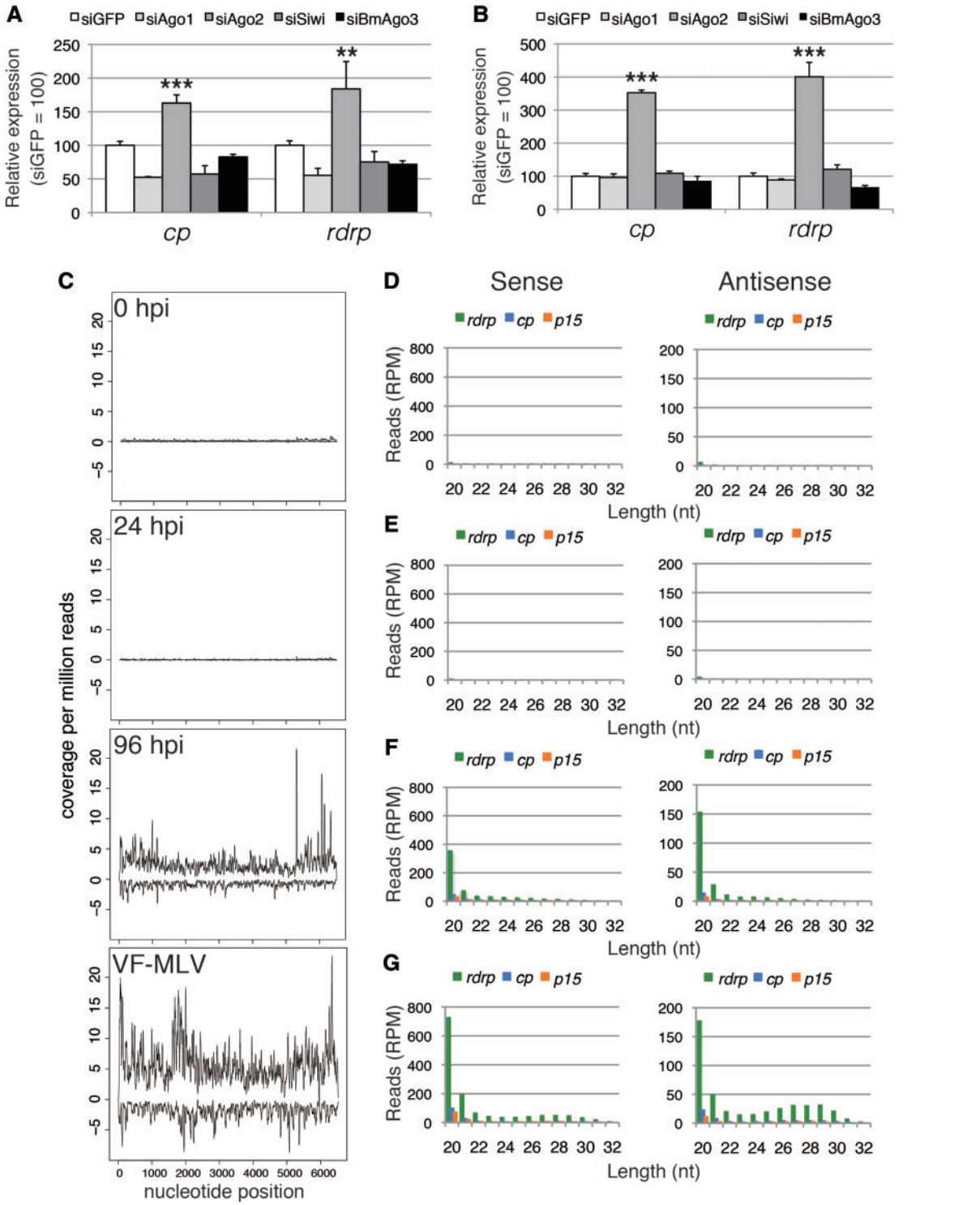

Figure 5. RNAi pathway alone suppresses BmMLV replication in VF cells. (A) Expression of *cp* and *rdrp* RNAs in *Ago*-knocked down VF cells infected transiently with BmMLV. (B) Expression of *cp* and *rdrp* RNAs in *Ago*-knocked down VF-MLV cells. Data represent the mean ± SD of triplicates. $^{**}P<0.01$, $^{***}P<0.001$ by one-way ANOVA and Dunnett's posttests using siGFP as a control. (C) Profiling of BmMLV RNA-derived small RNAs during acute infection in VF cells at 0, 24 and 96 hpi and persistent infection in VF-MLV cells. (D–G) Length distribution of BmMLV small RNAs in VF cells infected with BmMLV at 0 (D), 24 (E) and 96 (F) hpi, or in VF-MLV cells (G).

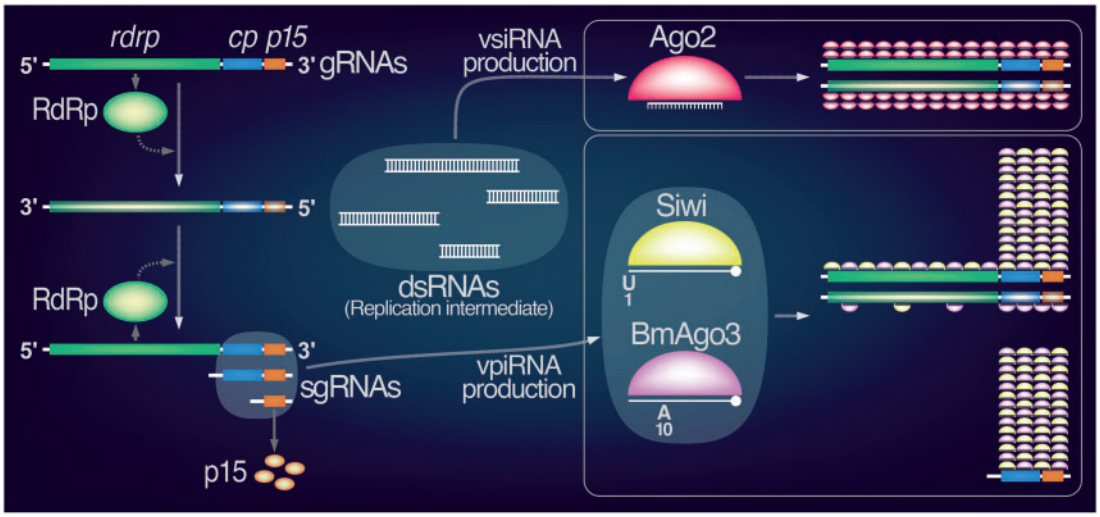

Figure 6. A proposed model for the molecular interaction between silkworm cells and BmMLV. Most virus-derived piRNA (vpiRNAs) are produced from sense subgenomic RNAs (sgRNAs), whereas virus-derived siRNAs (vsiRNAs) are generated from double-stranded BmMLV RNA-derived precursor RNAs. These small RNAs prevent lethal infection and allow the virus to establish a persistent infection. On the other hand, BmMLV utilizes p15 protein to propagate itself properly in silkworm cells in an unknown manner.

(Supplementary Fig. S3), which indicates that BmMLV accumulated in BmN-4 cells at about two times the level found in VF-MLV cells. It is possible to speculate that the silencing process against BmMLV developed in two steps: the first is a canonical siRNA-mediated pathway, and then the piRNA-mediated targeting begins when the virus load reaches a certain threshold during persistent infection. If this is the case, then BmMLV will be repressed by both vsiRNAs and vpiRNAs in VF-MLV cells in the future.

In general, the *de novo* production of piRNAs against exogenous elements is considered to require integration into the active piRNA clusters.[36–39] In this study, we detected BmMLV RNA-derived vpiRNAs in silkworm BmN-4 cells. Southern blotting and genomic PCR clearly demonstrated that the BmMLV genome is not integrated into the genomes of BmN-4,[2] which indicates that BmMLV RNA-derived vpiRNAs are produced in a non-canonical manner. Similar phenomena have been reported in *Drosophila* ovarian somatic sheet (OSS) cells,[40] *Aedes* mosquitoes and *Aedes* cell lines.[41–45] OSS cells expressed vpiRNAs for several persistently infected RNA viruses,[40] whereas *Drosophila* did not produce vpiRNA during both acute and persistent viral infections, and thus the piRNA pathway is not required for antiviral defense in adult *Drosophila*.[46] On the other hand, piRNA pathways play roles in silencing RNA viruses in both adult *Aedes* and *Aedes* cultured cells,[45] so the importance of vpiRNA production in antiviral defense systems even differs within the same order (Diptera). In the present study, we discovered that the piRNA pathway also functioned to combat an RNA virus in lepidopteran cultured cells. At present, it is unknown how the host cells recognize non-integrated exogenous elements and produce piRNAs against them, but silkworm and mosquito cells may provide useful systems for exploring this piRNA-mediated silencing mechanism.

In conclusion, the present study determined for the first time the molecular interaction between insect cells and a plant virus-like insect RNA virus. We identified both the host and viral factors that are required to establish persistent BmMLV infections in silkworm cultured cells. Silkworm cultured cells negatively regulate viral growth by siRNA and piRNA pathways, which may prevent lethal infection and allow the virus to establish a persistent infection. On the other hand, BmMLV utilizes a novel protein, p15, to propagate itself in insect cells in an unknown manner (Fig. 6). It would be very interesting to understand how the p15 protein controls the host cell machinery during the establishment of virus infections as well as the origin of this protein.

S.K. and M.I. conceived of and designed the experiments. S.K., K.S., T.A., M.O., T.M., H.K. and M.I. performed molecular biological experiments. M.K. and K.S. performed most of the bioinformatic analyses. N.I., S.S., Y.T. and Y.S. performed deep sequencing and data analysis. All of the authors discussed the data and helped for manuscript preparation. S.K. wrote the manuscript with intellectual input from all authors. S.K. and M.I. supervised the project.

Acknowledgements

We thank Kodai Uchiyama, Genki Ishihara and Daikichi Sakai for technical assistance.

Funding

This work was supported by JSPS KAKENHI grant numbers JP15H02482, JP16KT0064, and JP16H05051 to S.K., JP221S0002 to S.S. and Y.S., JP16K08095 and JP25450482 to M.I., JP17K17673 to N.I. and JP17J02408 to K.S. and MEXT KAKENHI grant number JP26113007 to Y.T. The funders had no role in study design, data collection and analysis, decision to publish, or preparation of the manuscript.

Conflict of interest

None declared.

Supplementary data

Supplementary data are available at *DNARES* online.

References

1. Martelli, G.P., Sabanadzovic, S., Abou Ghanem-Sabanadzovic, N. and Saldarelli, P. 2002, *Maculavirus*, a new genus of plant viruses, *Arch. Virol.*, **147**, 1847–53.

2. Katsuma, S., Tanaka, S., Omuro, N., et al. 2005, Novel macula-like virus identified in *Bombyx mori* cultured cells, *J. Virol.*, **79**, 5577–84.
3. King, A.M.Q., Adams, M.J., Carstens, E.B. and Lefkowitz, E.J. 2011, *Virus Taxonomy: Classification and Nomenclature of Viruses: Ninth Report of the International Committee on Taxonomy of Viruses*, pp. 944–952. Elsevier Academic Press, London.
4. Innami, K., Aizawa, T., Tsukui, T., et al. 2016, Infection studies of non-target mammalian cell lines with *Bombyx mori* macula-like virus, *J. Virol. Methods*., **229**, 24–6.
5. Iwanaga, M., Hitotsuyama, T., Katsuma, S., et al. 2012, Infection study of *Bombyx mori* macula-like virus (BmMLV) using a BmMLV-negative cell line and an infectious cDNA clone, *J. Virol. Methods*, **179**, 316–24.
6. Maeda, S. 1984, A plaque assay and cloning of *Bombyx mori* nuclear polyhedrosis virus, *J. Seric. Sci. Jpn*., **53**, 547–8.
7. Kiuchi, T., Koga, H., Kawamoto, M., et al. 2014, A single female-specific piRNA is the primary determiner of sex in the silkworm, *Nature*, **509**, 633–6.
8. Grabherr, M.G., Haas, B.J., Yassour, M., et al. 2011, Full-length transcriptome assembly from RNA-Seq data without a reference genome, *Nat. Biotechnol*., **29**, 644–52.
9. Li, B. and Dewey, C.N. 2011, RSEM: accurate transcript quantification from RNA-Seq data with or without a reference genome, *BMC Bioinform*., **12**, 323.
10. Anders, S. and Huber, W. 2010, Differential expression analysis for sequence count data, *Genome Biol*., **11**, R106.
11. Kim, D., Pertea, G., Trapnell, C., Pimentel, H., Kelley, R. and Salzberg, S.L. 2013, TopHat2: accurate alignment of transcriptomes in the presence of insertions, deletions and gene fusions, *Genome Biol*., **14**, R36.
12. Kawamoto, M., Koga, H., Kiuchi, T., et al. 2015, Sexually biased transcripts at early embryonic stages of the silkworm depend on the sex chromosome constitution, *Gene*, **560**, 50–6.
13. Izumi, N., Kawaoka, S., Yasuhara, S., et al. 2013, Hsp90 facilitates accurate loading of precursor piRNAs into PIWI proteins, *RNA*, **19**, 896–901.
14. Shoji, K., Suzuki, Y., Sugano, S., Shimada, T. and Katsuma, S. 2017, Artificial "ping-pong" cascade of PIWI-interacting RNA in silkworm cells, *RNA*, **23**, 86–97.
15. International Silkworm Genome Consortium. 2008, The genome of a lepidopteran model insect, the silkworm *Bombyx mori*, *Insect Biochem. Mol. Biol*, **38**, 1036–45.
16. Langmead, B., Trapnell, C., Pop, M. and Salzberg, S.L. 2009, Ultrafast and memory-efficient alignment of short DNA sequences to the human genome, *Genome Biol*., **10**, R25.
17. Li, H., Handsaker, B., Wysoker, A., et al. 2009, The sequence alignment/-map (SAM) format and SAMtools, *Bioinformatics*, **25**, 2078–9.
18. Quinlan, A.R. and Hall, I.M. 2010, BEDTools: a flexible suite of utilities for comparing genomic features, *Bioinformatics*, **26**, 841–2.
19. Shoji, K., Hara, K., Kawamoto, M., et al. 2014, Silkworm HP1a transcriptionally enhances highly expressed euchromatic genes via association with their transcription start sites, *Nucleic Acids Res*., **42**, 11462–71.
20. Mitsuhara, I., Ugaki, M., Hirochika, H., et al. 1996, Efficient promoter cassettes for enhanced expression of foreign genes in dicotyledonous and monocotyledonous plants, *Plant Cell Physiol*., **37**, 49–59.
21. Wang, W.Q., Natsuaki, T., Kosaka, Y. and Okuda, S. 2006, Comparison of the nucleotide and amino acid sequences of parental and attenuated isolates of *Zucchini yellow mosaic virus*, *J. Gen. Plant Pathol*., **72**, 52–6.
22. Hajdukiewicz, P., Svab, Z. and Maliga, P. 1994, The small, versatile pPZP family of Agrobacterium binary vectors for plant transformation, *Plant Mol. Biol*., **25**, 989–94.
23. Ruiz, M.T., Voinnet, O. and Baulcombe, D.C. 1998, Initiation and maintenance of virus-induced gene silencing, *Plant Cell*, **10**, 937–46.
24. Garrett, A.M., Tadenev, A.L. and Burgess, R.W. 2012, DSCAMs: restoring balance to developmental forces, *Front. Mol. Neurosci*., **5**, 86.
25. Elkins, T., Hortsch, M., Bieber, A.J., Snow, P.M. and Goodman, C.S. 1990, *Drosophila* fasciclin I is a novel hemophilic adhesion molecule that along with dasciclin III can mediate cell sorting, *J. Cell Biol*., **110**, 1825–32.
26. Li, F. and Ding, S.W. 2006, Virus counterdefense: diverse strategies for evading the RNA-silencing immunity, *Annu. Rev. Microbiol*., **60**, 503–31.
27. Johansen, L.K. and Carrington, J.C. 2001, Silencing on the spot. Induction and suppression of RNA silencing in the Agrobacterium-mediated transient expression system, *Plant Physiol*., **126**, 930–8.
28. Wang, L., Lv, X., Zhai, Y., et al. 2012, Genomic characterization of a novel virus of the family *Tymoviridae* isolated from mosquitoes, *PLoS One*, **7**, e39845.
29. de Miranda, J.R., Cornman, R.S., Evans, J.D., et al. 2015, Genome characterization, prevalence and distribution of a Macula-like virus from *Apis mellifera* and *Varroa destructor*, *Viruses*, **7**, 3586–602.
30. Zhu, L., Li, Z., Tatsuke, T., et al. 2013, Genome-wide identification of Argonaute 1- and Argonaute 2-regulating genes revealed an inhibition of macula-like virus by RNAi pathway in the silkworm, Bombyx mori, *J. Insect Biotech. Sericol*., **82**, 19–23.
31. Izumi, N., Shoji, K., Sakaguchi, Y., et al. 2016, Identification and functional analysis of the pre-piRNA 3′ Trimmer in silkworms, *Cell*, **164**, 962–73.
32. Hirose, T., Mishima, Y. and Tomari, Y. 2014, Elements and machinery of non-coding RNAs: toward their taxonomy, *EMBO Rep*., **15**, 489–507.
33. Nie, Z., Zhou, F., Li, D., et al. 2013, RIP-seq of BmAgo2-associated small RNAs reveal various types of small non-coding RNAs in the silkworm, *Bombyx mori*, *BMC Genomics*, **14**, 661.
34. Kawaoka, S., Hayashi, N., Suzuki, Y., et al. 2009, The *Bombyx* ovary-derived cell line endogenously expresses PIWI/PIWI-interacting RNA complexes, *RNA*, **15**, 1258–64.
35. Kawaoka, S., Minami, K., Katsuma, S., Mita, K. and Shimada, T. 2008, Developmentally synchronized expression of two *Bombyx mori* Piwi subfamily genes, *SIWI* and *BmAGO3* in germ-line cells, *Biochem. Biophys. Res. Commun*., **367**, 755–60.
36. Muerdter, F., Olovnikov, I., Molaro, A., et al. 2012, Production of artificial piRNAs in flies and mice, *RNA*, **18**, 42–52.
37. Kawaoka, S., Mitsutake, H., Kiuchi, T., et al. 2012, A role for transcription from a piRNA cluster in *de novo* piRNA production, *RNA*, **18**, 265–73.
38. Yamamoto, Y., Watanabe, T., Hoki, Y., et al. 2013, Targeted gene silencing in mouse germ cells by insertion of a homologous DNA into a piRNA generating locus, *Genome Res*., **23**, 292–9.
39. Shoji, K. and Katsuma, S. 2015, Is the expression of sense and antisense transgenes really sufficient for artificial piRNA production? *Curr. Biol*., **25**, R708–10.
40. Wu, Q., Luo, Y., Lu, R., et al. 2010, Virus discovery by deep sequencing and assembly of virus-derived small silencing RNAs, *Proc. Natl. Acad. Sci. USA*, **107**, 1606–11.
41. Morazzani, E.M., Wiley, M.R., Murreddu, M.G., Adelman, Z.N. and Myles, K.M. 2012, Production of virus-derived ping-pong-dependent piRNA-like small RNAs in the mosquito soma, *PLoS Pathog*., **8**, e1002470.
42. Scott, J.C., Brackney, D.E., Campbell, C.L., et al. 2010, Comparison of dengue virus type 2-specific small RNAs from RNA interference-competent and -incompetent mosquito cells, *PLoS Negl. Trop. Dis*., **4**, e848.
43. Vodovar, N., Bronkhorst, A.W., van Cleef, K.W., et al. 2012, Arbovirus-derived piRNAs exhibit a ping-pong signature in mosquito cells, *PLoS One*, **7**, e30861.
44. Léger, P., Lara, E., Jagla, B., et al. 2013, Dicer-2- and Piwi-mediated RNA interference in Rift Valley fever virus-infected mosquito cells, *J. Virol*., **87**, 1631–48.
45. Miesen, P., Girardi, E. and van Rij, R.P. 2015, Distinct sets of PIWI proteins produce arbovirus and transposon-derived piRNAs in *Aedes aegypti* mosquito cells, *Nucleic Acids Res*., **43**, 6545–56.
46. Petit, M., Mongelli, V., Frangeul, L., Blanc, H., Jiggins, F. and Saleh, M.C. 2016, piRNA pathway is not required for antiviral defense in *Drosophila melanogaster*, *Proc. Natl. Acad. Sci. USA*, **113**, E4218–27.